Effect of Blurring of Images on Their First Order Radiomic Features

Dmitrii Tumakov[1*], *Artur* Giniatullin[1], *Yulia* Mingazova[2]
[1]Institute of Computational Mathematics and Information Technologies, Kazan Federal University, Kazan, Russia
[2]Center for Strategic Assessments and Forecasts of the Institute of Management, Economics and Finance, Kazan Federal University, Kazan, Russia

Abstract. The effect of uniform blurring of images on their (statistical) radiomic features of the first order is studied. Two sets each consisting of 100 images with sizes of 100 by 100 and 700 by 700 are chosen as a dataset. Tables showing the effect of blurs on seventeen selected radiomic properties are given. The mean, variation and coefficient of variation of changes in the considered properties for various degrees of blurring are estimated. It is concluded that the most representative radiomic properties characterizing blurs are the mean, RMS and energy.

Keywords: Blurring of images · Numerous blurs · Radiomic features · First order radiomic · Statistical features.

1 Introduction

The analysis of transformed images is an important problem in the field of image processing and computer vision. Image blur is a common image transformation that can occur due to various effects such as subject or camera movement during shooting, incorrect focus, noise from the camera matrix, as well as other effects. Thus, blurring of images is a kind of "parasitic" process that makes the image less clear and reduces the level of detail [1].

Restoring a blurred image is a way to remove negative effects or, ideally, to restore the original noise-free image. This is a complex and time-consuming task, and for its implementation, it is required to understand what characteristics change when the image is blurred [2]. The most commonly used approach for blur removal is the minimization of a functional, which takes into account the characteristics that change during blurring.

To control and quantify the effect of image blurring, various blur metrics have been proposed. One of the first blur estimates [3] was developed in 1997 to improve image super-resolution algorithms, and then the blur estimate was used as a quality metric. In 1999, blurring was estimated using a histogram of Discrete Cosine Transform (DCT) coefficients [4]. Later, several metrics based on edge detection were proposed. Among them, in [5], the

* Corresponding author: dtumakov@kpfu.ru

blur index was presented without reference to images. This blur measure is based on an analysis of the spread of the edges of the image. In [6], a content-independent metric was developed, and the sharpness (inverse of blurring) was estimated by calculating the kurtosis of the DCT on blocks containing boundaries.

Various measures can be used to evaluate images such as blur measure, sharpness measure, etc [8]. For example, the blur measure proposed in [9] uses a low-pass filter and is based on the principle that the gray level of neighboring pixels in a less blurred image changes with more variation than its blurred copy.

To date, radiomic features are often used for image analysis to extract a large number of features in both medical images and images used in other fields. Radiomics is also frequently used in the detection of various visually detectable diseases and abnormalities [10, 11]. In addition, these features can be used in the study of their changes with various image transformations [12]. In practice, the pyRadiomics python package is often used for calculations of the features [13].

The Radiomics values not only indicate the quantitative histogram and texture characteristics of a medical image, but are also used as input data for machine learning [14-16]. Therefore, it is important to evaluate these parameters in blurred images in order to assess the degree of change of the original image.

In the present paper, 17 significant first-order statistical descriptors are selected from the total number of Radiomics, which are statistical features. The characteristic features of the change in the radiomic statistical parameters of images during blurring are revealed. The dependences of these parameters on the degree of blurring of the original images are determined. Tables are given showing the effect of blurring on the selected radiomic properties. Conclusions are drawn about the most revealing properties that characterize the degree of blurring.

2 Blurring of Images

Blurring of images (convolution from a mathematical point of view) is an image processing operation that allows applying a filter to an image by moving the filter (convolution matrix) over the entire image area [9].

Mathematically, convolution can be expressed through the following formula [1]:

$$g(x,y) = w * f(x,y) = \sum_{dx=-a}^{a} \sum_{dy=-b}^{b} w(dx,dy) f(x-dx, y-dy),$$

where $g(x,y)$ is image after applying convolution; w is convolution kernel; $f(x,y)$ is original image; a, b are specified convolution boundaries.

In the present paper, the convolution kernel is a 9×9 matrix, the main and secondary diagonals of which are filled with one, while the remaining elements of the matrix are zero (Figure 1).

$$\begin{pmatrix} 1 & 0 & 0 & 0 & 0 & 0 & 0 & 0 & 1 \\ 0 & 1 & 0 & 0 & 0 & 0 & 0 & 1 & 0 \\ 0 & 0 & 1 & 0 & 0 & 0 & 1 & 0 & 0 \\ 0 & 0 & 0 & 1 & 0 & 1 & 0 & 0 & 0 \\ 0 & 0 & 0 & 0 & 1 & 0 & 0 & 0 & 0 \\ 0 & 0 & 0 & 1 & 0 & 1 & 0 & 0 & 0 \\ 0 & 0 & 1 & 0 & 0 & 0 & 1 & 0 & 0 \\ 0 & 1 & 0 & 0 & 0 & 0 & 0 & 1 & 0 \\ 1 & 0 & 0 & 0 & 0 & 0 & 0 & 0 & 1 \end{pmatrix}$$

Fig. 1. The blur matrix

We will apply this matrix to images as a convolution, achieving the Motion Blur effect.

3 First Order Features of Radiomics

The first order statistic of radiomic features describes the distribution of pixel intensities in the region of the image defined by the mask using commonly used metrics. Let us list all these features.

Energy (E) is a measure of the magnitude of squares of the brightness values of pixels in an image. Brighter images provide greater energy. Energy is calculated using the following formula:

$$E = \sum_{i=1}^{N_p} \boldsymbol{X}(i)\,, \tag{1}$$

where N_p is total number of pixels; $\boldsymbol{X}(i)$ i-th pixel intensity. One can also use such a characteristic as the total energy, which takes into account the area of the pixel. Since the total energy and energy are proportional to each other, we will not consider the total energy, limiting ourselves to energy only.

Entropy (Ent) defines the uncertainty of image values. It measures the average amount of information needed to encode image values and is calculated by the formula:

$$Ent = -\sum_{i=1}^{N_g} p(i)\log_2(p(i)+\varepsilon), \tag{2}$$

where ε is small positive number ($\approx 2.2 \times 10^{-16}$); N_g is quantity of non-zero pixel intensity intervals. N_g can take a value of 256 (maximum) or smaller, depending on the selected histogram. In the present work, we will assume that $N_g = 256$. The $p(i)$ value is found as the number of points of a given intensity divided by the total number of pixels N_p, and represents a normalized first-order histogram.

Uniformity is a measure of the sum of squares of each intensity value. It is a measure of the uniformity of an image array, where a high value of uniformity implies a greater uniformity or a smaller range of discrete intensity values:

$$Uni = \sum_{i=1}^{N_p} p(i)^2\,. \tag{3}$$

Minimum (Min) and *maximum (Max)* are defined in a standard way. *The range of values (R)* that depends on the latter is defined as

$$R = Max - Min. \tag{4}$$

Despite the similarity of the formula with a formula for energy and due to the importance of this characteristic, we also define the *average intensity ($\bar{X}$)*

$$\bar{X} = \frac{1}{N_p}\sum_{i=1}^{N_p} \boldsymbol{X}(i)\,. \tag{5}$$

Median (Mdn) is the median value of all data arranged sequentially in ascending order.

Variance (Var) is the average of squares of distances of each intensity value from the mean value. It is a measure of the dispersion of a distribution about the mean and is determined through the following formula:

$$Var = \frac{1}{N_p}\sum_{i=1}^{N_p} (\boldsymbol{X}(i) - \bar{X})^2. \tag{6}$$

The standard deviation, like the variance, measures the amount of deviation from the mean and is calculated as the square root of the variance. We will not consider this value.

Mean Absolute Deviation (MAD) is the average distance of all intensity values from the mean value of the image array.

$$MAD = \frac{1}{N_p}\sum_{i=1}^{N_p} |\boldsymbol{X}(i) - \bar{X}|\,. \tag{7}$$

Root mean square (RMS) is the square root of the average of all squared intensity values:

$$RMS = \sqrt{\frac{1}{N_p}\sum_{i=1}^{N_p} \boldsymbol{X^2}(i)}\,. \tag{8}$$

Values such as percentiles are also evaluated. These are values that indicate the boundary of the division of a data set in such a way that a given percentage of all data has values less than a specified one. That is, the Nth percentile is a number such that N% of the array elements are less than or equal to this number. The *90th percentile ($\boldsymbol{P_{90}}$)* and the *10th percentile ($\boldsymbol{P_{10}}$)* are considered. The *interquartile range (Int)* is estimated as follows:

$$Int = \boldsymbol{P_{75}} - \boldsymbol{P_{25}}. \tag{9}$$

Here, $\boldsymbol{P_{75}}$ and $\boldsymbol{P_{25}}$ are the 75th and 25th percentiles of the pixel intensity sequence, respectively.

Robust mean absolute deviation (rMAD) is the average distance of all intensity values from the mean, calculated for a subset of the array of intensities with levels between the 10th and 90th percentiles:

$$rMAD = \frac{1}{N_{10-90}}\sum_{i=1}^{N_{10-90}} |\boldsymbol{X}_{10-90}(i) - \bar{X}_{10-90}|. \tag{10}$$

Skewness (Skew) measures the skewness of a distribution of values relative to the mean. Depending on where the tail is lengthened and the mass of the distribution is concentrated, this value can be positive or negative:

$$Skew = \frac{\frac{1}{N_p}\sum_{i=1}^{N_p}(\boldsymbol{X}(i) - \bar{X})^3}{\left(\sqrt{\frac{1}{N_p}\sum_{i=1}^{N_p}(\boldsymbol{X}(i) - \bar{X})^2}\right)^3}. \quad (11)$$

Kurtosis (Kurt) is a measure of the "peakiness" of the distribution of values in the histogram of image intensities. Higher kurtosis implies that the mass of the distribution is concentrated in the tail rather than in the mean. Smaller kurtosis implies the opposite, i.e. that the mass of the distribution is concentrated in the direction of the spike close to the mean:

$$Kurt = \frac{\frac{1}{N_p}\sum_{i=1}^{N_p}(\boldsymbol{X}(i) - \bar{X})^4}{\left(\frac{1}{N_p}\sum_{i=1}^{N_p}(\boldsymbol{X}(i) - \bar{X})^2\right)^2}. \quad (12)$$

Thus, in what follows, we will consider 17 statistical radiomic features.

4 Results

4.1 Dataset

To analyze the effect of blurs on the properties of radiomics, we use a set of 100 grayscale photographs of 100×100 pixels resolution from the site kaggle.com (https://storage.googleapis.com/kaggle-datasets/34662/46346/bundle/archive.zip?). These photos are then scaled up to a resolution of 700×700 pixels using the python *resize*() function from the PIL library. Thus, we obtain two sets of data. The same results were obtained for both data sets. In the present paper, we present the results for large images.

To study the effect of blurring, we apply the blur operation to the original images several times. An example of the original image and images with three and five blurs are shown in Figure 2.

Fig. 2. Photos with different degrees of blurring: no blur (left), 3 blurs (center), 5 blurs (right)

4.2 Changes in radiomics properties due to blurring

Let us apply the blur operation with the matrix shown in Figure 1 one, two, three, five, and ten times. Let us calculate the values of changes in the estimated radiomic parameters for all

100 images. For the obtained sets of blurred images, we calculate the mean, variation and coefficient of variation, which are presented in Tables 1-3, respectively.

Table 1. Changing the average depending on the degree of blurring.

Characteristics	1 blur	2 blurs	3 blurs	5 blurs	10 blurs
E	-0.061	-0.089	-0.108	-0.137	-0.194
Max	-0.018	-0.033	-0.042	-0.055	-0.08
R	-0.018	-0.033	-0.042	-0.055	-0.079
MAD	-0.049	-0.077	-0.092	-0.111	-0.137
RMS	-0.031	-0.046	-0.055	-0.071	-0.102
Var	-0.081	-0.129	-0.155	-0.188	-0.231
rMAD	-0.050	-0.079	-0.096	-0.116	-0.142
Ent	-0.012	-0.016	-0.017	-0.019	-0.022
Uni	0.074	0.102	0.1083	0.113	0.139
$\bar{X}$	-0.026	-0.036	-0.045	-0.06	-0.093
Mdn	-0.018	-0.028	-0.035	-0.051	-0.086
Int	-0.059	-0.091	-0.107	-0.129	-0.156
P_{10}	0.071	0.134	0.163	0.167	0.097
P_{90}	-0.038	-0.057	-0.069	-0.087	-0.117
Skew	-0.109	-0.181	-0.214	-0.246	-0.271
Kurt	0.037	0.057	0.067	0.077	0.087

Table 1 shows that the values for all properties except for uniformity, the 10th percentile and kurtosis are negative and decrease with the number of blurs. The increasing of blurring also causes all properties to increase in absolute value, except for the 10th percentile. Thus, all radiomics, except for the 10th percentile, can be used as comparative characteristics for assessing image blurring.

Table 2. Changing the variance depending on the degree of blurring.

Characteristics	1 blur	2 blurs	3 blurs	5 blurs	10 blurs
E	0.0003	0.00063	0.00085	0.00120	0.00189
Max	0.0012	0.00204	0.00254	0.00344	0.00477
R	0.0012	0.00205	0.00255	0.00345	0.00478
MAD	0.0010	0.00173	0.00226	0.00302	0.00427
RMS	0.00009	0.00018	0.00024	0.00036	0.00061
Var	0.0034	0.00535	0.00666	0.00850	0.01139
rMAD	0.0013	0.00215	0.00276	0.00367	0.00538
Ent	0.00006	0.00011	0.00016	0.00024	0.00043
Uni	0.0144	0.02124	0.02950	0.03384	0.05525
$\bar{X}$	0.00002	0.00003	0.00005	0.00008	0.00023
Mdn	0.0004	0.00090	0.00107	0.00132	0.00199
Int	0.0024	0.00484	0.00654	0.00899	0.01237
P_{10}	0.0242	0.05214	0.08106	0.10937	0.13710
P_{90}	0.0008	0.00158	0.00202	0.00270	0.00375
Skew	1.1461	1.61679	2.06683	2.64040	3.25457
Kurt	0.0036	0.00628	0.00860	0.01251	0.02023

Dispersion as an indicator characterizes how much the changes in the values of radiomic properties differ for different images. Namely, a large dispersion indicates that the behavior of the values for different images can quantitatively differ. For all characteristics, an increase in dispersion with an increase in blurring is clearly visible. However, a quantitative comparison of the dispersion values between different properties does not make sense, since the values themselves can differ significantly. To compare different values, we use the coefficient of variation (Table 3).

Table 3. Changing the coefficient of variation depending on the degree of blurring.

Characteristics	1 blur	2 blurs	3 blurs	5 blurs	10 blurs
E	0.301	0.281	0.268	0.25	0.224
Max	1.917	1.361	1.182	1.052	0.86
R	1.970	1.381	1.195	1.06	0.865
MAD	0.649	0.541	0.513	0.491	0.474
RMS	0.308	0.289	0.278	0.263	0.24
Var	0.725	0.565	0.523	0.49	0.46
rMAD	0.718	0.584	0.546	0.521	0.514
Ent	0.639	0.679	0.722	0.79	0.909
Uni	1.623	1.435	1.585	1.618	1.684
$\bar{X}$	0.157	0.151	0.149	0.152	0.163
Mdn	1.149	1.058	0.909	0.702	0.512
Int	0.833	0.768	0.751	0.729	0.71
P_{10}	2.199	1.708	1.742	1.974	3.803
P_{90}	0.749	0.693	0.651	0.595	0.52
Skew	9.829	7.041	6.716	6.589	6.647
Kurt	1.624	1.392	1.38	1.437	1.619

The values presented in Table 3 can be compared with each other. It can be seen that the following characteristics have the smallest relative changes: *E*, *RMS* and $\bar{X}$. Their values do not exceed 0.5. However, only the average pixel intensity has an average spread. Almost all quantities with coefficients of variation less than unity decrease with an increase in blurring, thus characterizing stable behavior for strong blurs. Only the entropy values increase.

Thus, the properties of radiomics *E*, *RMS* and $\bar{X}$ can be considered the most indicative for characterizing the degree of blur. Let us draw plots of dependence of these properties on the degree of blurring (Figure 3).

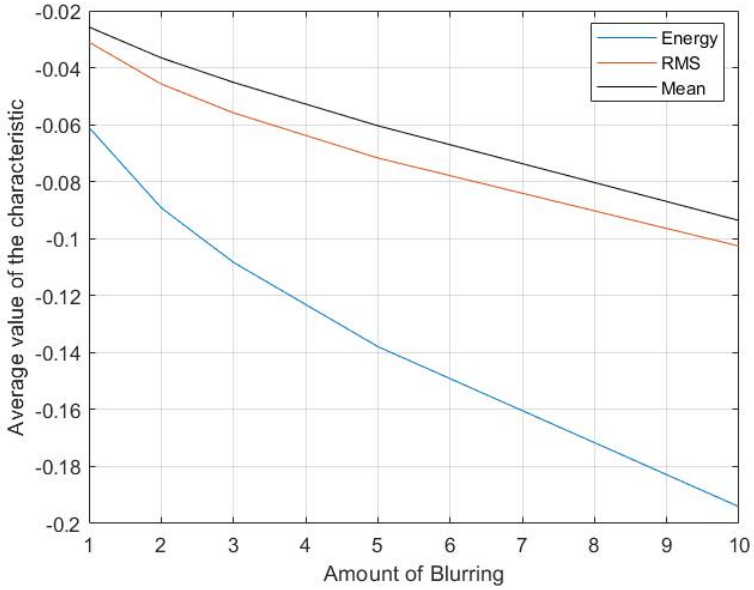

Fig. 3. Dependence of energy (blue), mean (black) and root mean square (orange) on the amount of blurring.

5 Conclusion

To analyze the effect of blurs on images, we selected two sets each containing 100 images with sizes of 100 by 100 and 700 by 700. Characteristic features of the change in the radiomic statistical parameters of images during blurring are shown. The dependences of these parameters on the degree of image blurring are determined. It is concluded that the most indicative properties characterizing the degree of blurring are the average, RMS and energy.

The results obtained in the work can be used to estimate the degree of blurring of images and to restore blurred images when building objective functions or controlling image quality.

The work was funded by the subsidy allocated to Kazan Federal University for the state assignment in the sphere of scientific activities under the project no. FZSM – 2023 – 0017 "The economy of import substitution of the region in the conditions of transformation of logistics chains and deglobalization".

References

1. R.C. Gonzales, R.E. Woods, Digital Image Processing (2018)
2. G.N. Kislyansky, E.S. Nestrugina, *Restoration of defocused and blurred images,* Bulletin of Donetsk National University, Series G: Technical Sciences **4**, 41-53. – EDN MUFFIG (2020)
3. K. Zeng, Y. Wang, J. Mao, J. Liu, W. Peng and N. Chen, *A local metric for defocus blur detection based on CNN feature learning*, in IEEE Transactions on Image Processing, **28**, no. 5, pp. 2107-2115, May 2019, (2019)

4. G. Wang, Z. Wang, K. Gu, L. Li, Z. Xia and L. Wu, *Blind quality metric of DIBR-synthesized images in the discrete wavelet transform domain*, in IEEE Transactions on Image Processing, **29**, pp. 1802-1814, 2020, (2020)
5. B.E. Boult, M.C. Chiang, *Local blur estimation and super-resolution.* In Proc. IEEE, Computer Society Conference on Computer Vision and Pattern Recognition, pp. 821-826, June 1997, (1997)
6. X. Marichal, Wei-Ying Ma, H.J. Zhang, *Blur determination in the compressed domain using DCT information.* In Proc. IEEE, International Conference on Image Processing, 2:386–390, October 1999 (1999)
7. P. Marziliano, F. Dufaux, S. Winkler T. Ebrahimi, *A no-reference perceptual blur metric.* In Proc. IEEE, International Conference on Image Processing, 3:57–60, June 2002, (2002)
8. Dolmiere T., Ladret P. Crete F, *The blur effect: Perception and estimation with a new no-reference perceptual blur metric*. SPIE Electronic Imaging Symposium. Conference: Human Vision and Electronic Imaging, (2007)
9. J. Caviedes, S. Gurbuz, *No-reference sharpness metric based on local edge kurtosis.* In Proc. IEEE, International Conference on Image Processing, 3:53–56, June 2002, (2002)
10. A. Stefano, A. Leal, S. Richiusa, P. Trang, A. Comelli, V. Benfante, S. Cosentino, M.G. Sabini, A. Tuttolomondo, R. Altieri, F. Certo, G.M.V. Barbagallo, M. Ippolito, G. Russo, *Robustness of PET radiomics features: Impact of co-registration with MRI.* Applied Sciences **11**(21), 10170 (2021)
11. V. Benfante, A. Stefano, A. Comelli, P. Giaccone, F.P. Cammarata, S. Richiusa, F. Scopelliti, M. Pometti, M. Ficarra, S. Cosentino, M. Lunardon, F. Mastrotto, A. Andrighetto, A. Tuttolomondo, R. Parenti, M. Ippolito, G. Russo, *A new preclinical decision support system based on PET radiomics: A preliminary study on the evaluation of an innovative 64Cu-labeled chelator in mouse models*. Journal of Imaging **8**(4): 92 (2022)
12. D. Tumakov, Z. Kayumov, A. Zhumaniezov, D. Chikrin, D. Galimyanov, *Elimination of defects in mammograms caused by a malfunction of the device matrix*. Journal of Imaging **8**(5):128 (2022)
13. J.J.M. van Griethuysen, A. Fedorov, C. Parmar, A. Hosny, N. Aucoin, V. Narayan, R.G.H Beets-Tan, J.C. Fillion-Robin, S. Pieper, H.J.W.L Aerts, *Computational radiomics system to decode the radiographic phenotype*. Cancer Research **77**(21), 104-107 (2017)
14. M. Iori, C. Di Castelnuovo, L. Verzellesi, G. Meglioli, D.G. Lippolis, A. Nitrosi, F. Monelli, G. Besutti, V. Trojani, M. Bertolini, A. Botti, G. Castellani, D. Remondini, R. Sghedoni, S. Croci, C. Salvarani, *Mortality prediction of COVID-19 patients using radiomic and neural network features extracted from a wide chest X-ray sample size: A robust approach for different medical imbalanced scenarios.* Applied Sciences 2022, **12**(8), 3903 (2022)
15. P. Alongi, R. Laudicella, F. Panasiti, A. Stefano, A. Comelli, P. Giaccone, A. Arnone, F. Minutoli, N. Quartuccio, C. Cupidi, G. Arnone, T. Piccoli, L.M.E Grimaldi, S. Baldari, G. Russo, *Radiomics analysis of brain [18F]FDG PET/CT to predict Alzheimer's disease in patients with amyloid PET positivity: A preliminary report on the application of SPM cortical segmentation, pyradiomics and machine-learning analysis.* Diagnostics **12**(4), 933 (2022)
16. I. Daimiel Naranjo, P. Gibbs, J.S. Reiner, R. Lo Gullo, S.B. Thakur, M.S. Jochelson, N. Thakur, P.A.T. Baltzer, T.H. Helbich, K. Pinker*, Breast lesion classification with multiparametric breast MRI using radiomics and machine learning: A comparison with radiologists' performance.* Cancers **14**(7), 1743 (2022)